ELSEVIER

www.elsevier.nl/locate/carres

Carbohydrate Research 331 (2001) 173–182

CARBOHYDRATE RESEARCH

Structure of the exopolysaccharide produced by *Streptococcus thermophilus* S3

Elisabeth J. Faber, Mischa J. van den Haak, Johannis P. Kamerling,* Johannes F.G. Vliegenthart

Department of Bio-Organic Chemistry, Bijvoet Center, Utrecht University, PO Box 80.075, NL-3508 TB Utrecht, The Netherlands

Received 16 October 2000; accepted 9 January 2001

Abstract

The exopolysaccharide of *Streptococcus thermophilus* S3, produced in skimmed milk, is composed of D-galactose and L-rhamnose in a molar ratio of 2:1. The polysaccharide contains 0.4 equiv of *O*-acetyl groups per repeating unit. Linkage analysis and 1D/2D NMR (^{1}H and ^{13}C) studies on native and O-deacetylated EPS together with nanoES-CID tandem mass spectrometry studies on oligosaccharides generated by a periodate oxidation protocol, show the polysaccharide to have the following structure:

β-D-Gal*f*2Ac$_{0.4}$
1
↓
6
→3)-β-D-Gal*p*-(1→3)-α-D-Gal*p*-(1→3)-α-L-Rha*p*-(1→2)-α-L-Rha*p*-(1→2)-α-D-Gal*p*-(1→

Keywords: Lactic acid bacteria; Exopolysaccharide; *Streptococcus thermophilus*; Structural analysis

1. Introduction

In the food industry, microbial exopolysaccharides (EPSs) are widely applied as thickening, gelling and stabilizing agents.[1] Lactic acid bacteria, which carry the GRAS (generally recognized as safe) status, are excellent sources of such food grade exopolysaccharides. For example, when applied in food fermentation, the in situ production of exopolysaccharides will contribute to the texture of the product.

In order to initiate studies that may provide a better insight into the relationship between the structure of polysaccharides from lactic acid bacteria and the consistency of fermented products, detailed structural investigations have been performed on exopolysaccharides produced by different bacterial strains including *Lactobacillus acidophilus*,[2] *Lactobacillus delbrueckii* subsp. *bulgaricus* rr,[3] *Lactobacillus helveticus*,[4–8] *Lactobacillus paracasei*,[9] *Lactobacillus reuteri*,[10] *Lactobacillus rhamnosus*,[11] *Lactobacillus sake*,[12] *Lactococcus lactis* subsp. *cremoris*,[13,14] and *Streptococcus thermophilus*.[15–18]

S. thermophilus strains in combination with *Lb. delbrueckii* subsp. *bulgaricus* strains are used as commercial yogurt starters. The structure of their exopolysaccharides, as well as the

* Corresponding author. Tel.: +31-30-2533479; fax: +31-30-2540980.

E-mail address: kame@boc.chem.uu.nl (J.P. Kamerling).

0008-6215/01/$ - see front matter © 2001 Elsevier Science Ltd. All rights reserved.
PII: S0008-6215(01)00013-1

rheological properties of their subsequent yogurt gels, are studied in order to unravel the mechanisms by which the cultures and their exopolysaccharides influence the consistency of the yogurt.[18]

Here, we report the structural determination of the exopolysaccharide produced by the highly ropy *S. thermophilus* S3 strain in skimmed milk.

2. Results and discussion

Isolation, purification, and composition of the polysaccharides.—The exopolysaccharide, produced by *S. thermophilus* S3 in pasteurized reconstituted skimmed milk, was isolated, and purified via ethanol precipitation followed by acetone precipitation. The purity of the polysaccharide was confirmed by ^{1}H NMR spectroscopy (vide infra). From the *S. thermophilus* S3 culture, 36 mg/L of polysaccharide with an average molecular mass of 5.9×10^3 kDa was isolated.

Monosaccharide analysis of the native polysaccharide (n-EPS), including the determination of absolute configurations, revealed the presence of D-Gal and L-Rha in a molar ratio of 2:1. Methylation analysis of n-EPS (Table 1) demonstrated the presence of 2- and 3-substituted Rha*p*, 2-, 3-, and 3,6-substituted Gal*p* and terminal Gal*f* in equal molar amounts, indicating a branched hexasaccharide repeating unit. To determine the position of the acid-labile terminal Gal*f* residue, n-EPS was treated with 0.3 M trifluoroacetic acid (20 min, 100 °C), then subjected to methylation analysis (hyp-EPS). A 70% conversion of 3,6-substituted Gal*p* into 3-substituted Gal*p*, together with a decrease in the amount of terminal Gal*f* (Table 1), demonstrated that in the native polysaccharide, the terminal Gal*f* residue is attached to O-6 of the 3,6-substituted Gal*p* residue. The terminal Gal*p* derivative observed in the methylation analysis of the hydrolyzed sample originates from hydrolytically released Gal*f*.

Table 1
Methylation analysis data of *S. thermophilus* S3 native EPS (n-EPS), O-deacetylated EPS (dAc-EPS), and n-EPS after mild acid hydrolysis (hyd-EPS)

Derivative	Molar amounts [a]		
	n-EPS	dAc-EPS	hyd-EPS
2,3,5,6-Gal [b]	0.9	0.9	0.4
2,3,4,6-Gal			0.7
3,4,6-Gal	1.0	1.0	1.0
2,4,6-Gal	1.0	1.0	1.7
2,4-Gal	1.0	1.0	0.3
3,4-Rha	1.0	1.0	1.0
2,4-Rha	1.0	1.1	0.9

[a] 3,4,6-Gal is taken as 1.0.

[b] 2,3,5,6-Gal = 1,4-di-*O*-acetyl-2,3,5,6-tetra-*O*-methyl-galactitol-1-*d*, etc.

Treatment of n-EPS with 5% (w/v) NH_4OH at room temperature resulted in complete O-deacetylation of the polysaccharide (dAc-EPS), as determined by ^{1}H NMR spectroscopy (vide infra). Monosaccharide and methylation analysis (Table 1) indicated no additional changes of the O-deacetylated polysaccharide.

The 1D ^{1}H NMR spectrum of n-EPS (Fig. 1(A)) shows a complex signal pattern in terms of peak intensities in the anomeric region (δ 5.4–4.5) due to partial O-acetylation (*O*-acetyl, δ 2.148). After O-deacetylation of the polysaccharide (dAc-EPS), the pattern changes into five anomeric signals (Fig. 1(B)), of which the signal at $\delta \sim 5.16$ represents two anomeric protons, indicating a hexasaccharide repeating unit. A distinction between the anomeric signal of residue **D** (δ 5.16) and residue **E** (δ 5.17) could be made in the TOCSY spectra (vide infra). Furthermore, high-field signals ($\delta \sim 1.3$) are present, arising from the methyl groups of Rha*p* residues. The partial O-acetylation in n-EPS is reflected in the 1D ^{1}H NMR spectrum of n-EPS by an additional signal in the anomeric region at δ 4.958 for the proton at the O-acetylated carbon and a broadening of the anomeric signal at $\delta \sim 5.16$ originating from a contribution of H-1 of the O-acetylated residue. Based on integration of the anomeric signals in the spectrum, the extent of O-acetylation was determined to be 0.4 equiv. However, it must be kept in mind that the procedure used for the isolation of the polysaccharide may have resulted in partial O-deacetylation. The resolu-

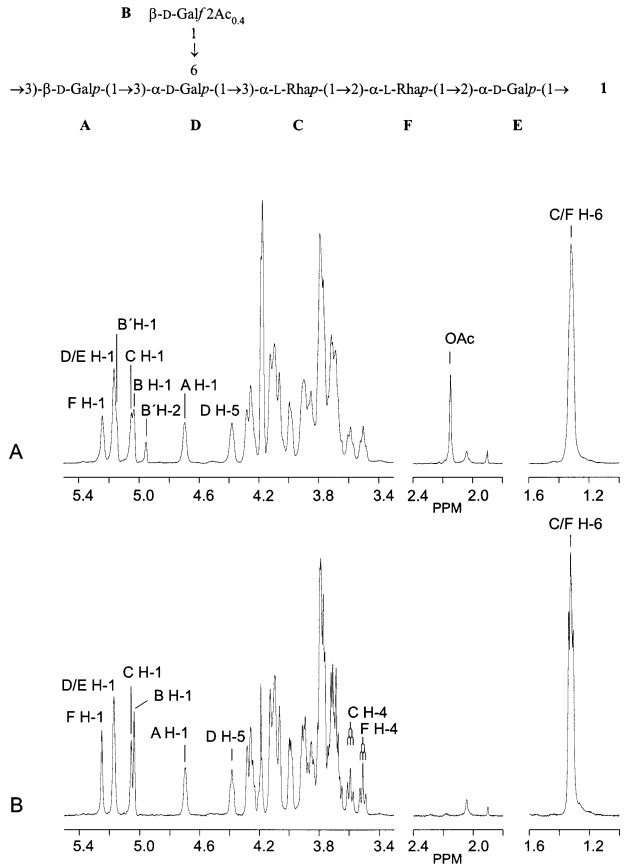

Fig. 1. 500-MHz ^{1}H NMR spectra of n-EPS **1** (A), and dAc-EPS **2** (B) produced by *S. thermophilus* S3, recorded in D_2O at 80 °C.

tion of the dAc-EPS spectrum (Fig. 1(B)) is higher than the resolution of the n-EPS spectrum (Fig. 1(A)).

For the assignment of the acetylated hexasaccharide repeating unit, the constituting residues are labeled **A**–**F** according to the increasing chemical shift values of the anomeric protons.

By making use of the 1D ^{1}H NMR spectrum, the 2D ^{13}C–^{1}H HSQC spectrum of dAc-EPS (vide infra) allowed the assignment of the chemical shifts of the corresponding anomeric carbon signals. The spectrum contains of six anomeric signals at δ 96.0 (residue **E**, $^1J_{C\text{-}1,H\text{-}1}$ 176 Hz), δ 97.0 (residue **D**, $^1J_{C\text{-}1,H\text{-}1}$ 171 Hz), δ 100.9 (residue **F**, $^1J_{C\text{-}1,H\text{-}1}$ 177 Hz), δ 102.4 (residue **C**, $^1J_{C\text{-}1,H\text{-}1}$ 174 Hz), δ 104.8 (residue **A**, $^1J_{C\text{-}1,H\text{-}1}$ 163 Hz), and δ 108.1 (residue **B**, $^1J_{C\text{-}1,H\text{-}1}$ 177 Hz), respectively, confirming the proposed hexasaccharide repeating unit. Based on the observed $^1J_{C\text{-}1,H\text{-}1}$ values, it could be deduced that residue **A** has the β anomeric configuration, whereas residues **C**, **D**, **E** and **F** have the α anomeric configurations. The relatively large $^1J_{C\text{-}1,H\text{-}1}$ values of residues **E** and **F** have been reported before for 2-substituted monosaccharides.[18] Since residue **B** is a Gal*f* residue (vide infra), $^1J_{C\text{-}1,H\text{-}1}$ will give no information about the anomeric configuration of the residue.

Periodate oxidation.—The methylated material, obtained after periodate oxidation of n-EPS and subsequent reduction ($NaBH_4$), methylation (CH_3I), mild acid hydrolysis, reduction ($NaBD_4$), and methylation (CD_3I), was dissolved in a water–methanol mixture and analyzed by nanoES-CID tandem mass spectrometry. In the high-mass region of the ES mass spectrum, an $[M + Na]^+$ ion at m/z 837 was detected, corresponding to an O-permethylated alditol ($Hex_2Pen_1Deoxyhex_1$)-1-*d* containing three deuterated methyl groups. The tandem mass spectrum obtained on collision activation of m/z 837 (Fig. 2) contains sodium-cationized $\mathbf{Y_n}$ fragments at m/z 252,

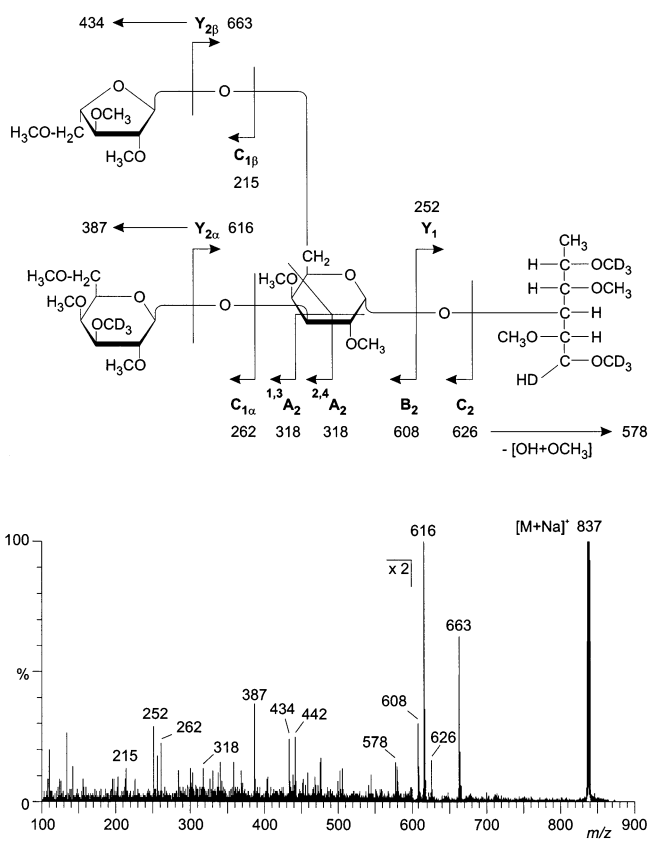

Fig. 2. Positive-ion mode nanoES-CID tandem mass spectrum of sodiated ions of the tetrasaccharide product obtained by a periodate oxidation protocol.

616, and 663 and sodium-cationized $\mathbf{C_n}$ fragments at m/z 215, 262, and 626. The $\mathbf{Y_1}$ ion at m/z 252 suggests the presence of a deoxyhexitol-1-*d* containing two deuterated methyl groups at the reducing end of the oligosaccharide. The signals at m/z 616 and 663, corresponding to the $\mathbf{Y_{2\alpha}}$ and $\mathbf{Y_{2\beta}}$ ions, respectively, are indicative of a disubstituted hexose linked to the deoxyhexitol-1-*d*, and thus reflect a branched structure. The $\mathbf{C_{1\alpha}}$ ion at m/z 262 corresponds to a terminal hexose containing one deuterated methyl group and the $\mathbf{C_{1\beta}}$ ion at m/z 215 corresponds to a terminal pentose. In view of the monosaccharide and methylation analysis data (vide supra), the pentose has to originate from the Gal*f* residue since selective degradation of the side chain of Gal*f* by periodate oxidation followed by reduction results in the formation of Ara*f*.[19] Secondary fragment ions are observed at m/z 387, 434, and 442. The ion at m/z 387 results from the loss of (deutero)methylated deoxyhexitol-1-*d* from the $\mathbf{Y_{2\alpha}}$ ion (m/z 616–229), while the ion at m/z 434 results from the loss of (deutero)methylated deoxyhexitol-1-*d* from the $\mathbf{Y_{2\beta}}$ ion (m/z 663–229). The ion at m/z 442 is the result of the loss of a terminal methylated pentose and a terminal (deutero)-methylated hexose from the pseudo-molecular ion (m/z 837–174–221). Furthermore, the ion at m/z 578 results from the loss of a hydroxy group at C-1 and an *O*-methyl group at C-2 forming a double bond between C-1 and C-2 at the reducing end of the $\mathbf{C_2}$ ion ($\mathbf{C_2}$–[OH + OCH_3]).[20]

In addition to ions resulting from the cleavage of glycosidic linkages ($\mathbf{C_n}$ and $\mathbf{Y_n}$), $^{1,3}\mathbf{A_2}$ and $^{2,4}\mathbf{A_2}$ ions resulting from cross-ring cleavage, are observed at m/z 318. The number of ions obtained from cross-linkage cleavages in this spectrum is insufficient to assign linkage types. However, combining methylation analysis data (vide supra) and the knowledge that periodate oxidation causes cleavage of 1,2-diol groups in 2-linked residues, provides proof for the selective removal of the 2-linked residues, leaving three 3-linked residues and a 6-linked terminal Gal*f*.

The results obtained from the ES-MS/MS spectrum together with those from the monosaccharide and methylation analyses performed on n-EPS, allowed the partial structure to be formulated as:

D-Gal*f*
1
↓
6
→3)-D-Gal*p*-(1→3)-D-Gal*p*-(1→3)-L-Rha*p*-(1→

In view of the final structure (vide infra), one would expect the isolated tetrasaccharide to contain an additional glycerol group at the reducing end. The absence of this group is due to the hydrolysis of the labile rhamnosyl glyceraldehyde linkage in the reduced and O-permethylated periodate-oxidized material.

In addition to the $[M + Na]^+$ ion at m/z 837 originating from the tetrasaccharide-alditol as illustrated above, the ES mass spectrum revealed amongst others, $[M + Na]^+$ ions at m/z 503, 506, 677, and 680. The tandem mass spectrum obtained from the $[M + Na]^+$ ion at m/z 677 contains sodium-cationized $\mathbf{Y_n}$ fragments at m/z 252 and 456 and sodium-cationized $\mathbf{C_n}$ fragments at m/z 262 and 466, indicating an O-permethylated alditol ($Hex_2Deoxyhex_1$)-1-*d* containing three deuterated methyl groups. Furthermore, the tandem mass spectrum obtained from the $[M + Na]^+$ ion at m/z 680 reveals sodium-cationized $\mathbf{Y_n}$ fragments at m/z 252 and 459 and sodium-cationized $\mathbf{C_n}$ fragments at m/z 262 and 469, indicating a O-permethylated alditol ($Hex_2Deoxyhex_1$)-1-*d* containing four deuterated methyl groups. Taking into account the tetrameric product generated by the periodate oxidation protocol (vide supra), the compound with a sodium-cationized ion at m/z 677 may result from the cleavage of the Sug*f*-(1 → 6)-Gal*p* (Sug = Gal or periodate-oxidized Gal) glycosidic linkage during periodate oxidation (pH ~4.0) and the subsequent addition of a methyl group at O-6 of the Gal*p* residue, whereas the compound having a $[M + Na]^+$ ion at m/z 680 may be formed by cleavage of the Ara*f* residue during the mild acid hydrolysis step and the subsequent addition of a deuterated methyl group.

The tandem mass spectrum obtained from the $[M + Na]^+$ ion at m/z 503 showed a sodium-cationized fragment $\mathbf{B_1}$ at m/z 244, $\mathbf{C_1}$ at m/z 262, and $\mathbf{Y_1}$ at m/z 282, corresponding to an O-permethylated alditol (Hex_2)-1-*d* containing three deuterated methyl groups. Fur-

thermore, the tandem mass spectrum obtained from the $[M + Na]^+$ ion at m/z 506 showed a sodium-cationized $\mathbf{B_1}$ fragment at m/z 244, a sodium-cationized $\mathbf{C_1}$ fragment at m/z 262, and an $\mathbf{Y_1}$ ion at m/z 285 indicating an O-permethylated alditol (Hex_2)-1-*d* containing four deuterated methyl groups. The disaccharide fragments with $[M + Na]^+$ ions at m/z 503 and m/z 506 originate from the tetrameric product with additional cleavage of the 6-linked residue during the periodate oxidation or during the succeeding mild acid hydrolysis step, respectively, and with cleavage of the Rha residue at the reducing end during the mild acid hydrolysis step.

2D NMR spectroscopy.—Assignments of the ^{1}H chemical shifts of n-EPS and dAc-EPS (Table 2) were performed by means of 2D TOCSY (mixing times 20, 75, and 150 ms) and 2D NOESY experiments. Starting points for the interpretation of the spectra were the H-1 signals of residues **A**–**F** and the methyl signals of residues **C** and **F**. Comparison of TOCSY spectra with increasing mixing times allowed the assignment of the sequential order of the chemical shifts belonging to a single spin system.

In the TOCSY spectra of dAc-EPS, the **A** H-2,3,4 resonances could be assigned on the TOCSY **A** H-1 track (δ 4.696). The observation of an intraresidual connectivity **A** H-1,H-3 in the NOESY spectrum (vide infra) at 3.78 ppm confirmed the overlap of the **A** H-2 and **A** H-3 resonances. The intraresidual **A** H-1,H-5 contact in the NOESY spectrum allowed the assignment of **A** H-5. The resonances of **A** H-6a,6b were assigned via their correlation to the corresponding ^{13}C resonance in the ^{13}C–^{1}H HSQC spectrum (vide infra). The TOCSY **B** H-1 track (δ 5.031) contains the complete series of cross-peaks with **B** H-2,3,4,5,6a,6b. On the TOCSY **D** H-1 track (δ 5.16), cross-peaks with **D** H-2,3,4 were observed. The **D** H-5 resonance was assigned through a cross-peak with **D** H-4 on the TOCSY **D** H-5 track (δ 4.382) and was confirmed in the NOESY spectrum (vide infra). The **D** H-6a,6b resonances were assigned through cross-peaks on the TOCSY **D** H-5 track (δ 4.382). All resonances of residue **E** (H-2,3,4,5,6a,6b) could be assigned on the TOCSY **E** H-1 track (δ 5.17). Beside it, the **E** (H-5,6a,6b) signals are clearly visible on the TOCSY **E** H-5 track (δ 4.24). The H-1,2,3,4,5 resonances of residues **C** and **F** could be assigned via their TOCSY C-6 track (**C** H-6 δ 1.31, **F** H-6 δ 1.33).

The assigned ^{1}H chemical shifts, in combination with the monosaccharide and methylation analysis data demonstrated **C** and **F** to be the Rha*p* residues; their H-6 signals are characteristic for 6-deoxy-hexose. Furthermore, the characteristic downfield chemical shifts of the H-4 signals of **A**, **D**, and **E** indicated these residues to represent Gal*p*, leaving residue **B** to be the Gal*f* residue.

Assignments of the ^{1}H chemical shifts of n-EPS (Table 2) were performed in essentially the same way as described for dAc-EPS. In addition, the **B′** H-1,3,4,5,6a,6b resonances of n-EPS could be assigned from the TOCSY **B′** H-2 track (δ 4.958). The differences in chemical shifts between **B** and **B′** H-1 ($\Delta\delta$ +0.12), **B** and **B′** H-2 ($\Delta\delta$ +0.87), and **B** and **B′** H-3 ($\Delta\delta$ +0.16), and the similarity of the chemical shifts of **B** and **B′** H-4,5,6a,6b (within $\Delta\delta$ 0.06) demonstrate that n-EPS is acetylated at O-2 of residue **B**.

The 2D ^{13}C–^{1}H HSQC spectra of both dAc-EPS (Fig. 3) and n-EPS (data not shown) allowed the assignment of the ^{13}C chemical shifts and coupling constants (Table 2). It should be noted that the intense signal at δ 61.4 reflects two C-atoms, namely **E** C-6 (deduced via **E** H-6a,6b) and **A** C-6. Using the position of **A** C-6, the proton signals of **A** H-6a,b, which could not be allocated in the TOCSY and NOESY spectra, were assigned. By comparing the carbon chemical shifts of the polysaccharide with literature data of methyl aldosides,[21] the linkage pattern of the individual residues was determined. In case of dAc-EPS, residue **A** could be assigned as the 3-substituted β-Gal*p* unit, since **A** C-3 (δ 78.5) has shifted downfield in comparison to β-D-Gal*p*1Me ($\delta_{C\text{-}3}$ 73.8). The upfield shift of **A** C-4 (δ 66.1) in comparison to β-D-Gal*p*1Me ($\delta_{C\text{-}4}$ 69.7) has been reported before for a 3-substituted β-D-Gal*p* glycoside.[22] Comparison of the ^{13}C chemical shifts of residue **B** with chemical shifts of α-D-Gal*f*1Me ($\delta_{C\text{-}1}$ 103.8, $\delta_{C\text{-}2}$ 78.2, $\delta_{C\text{-}3}$ 76.2, $\delta_{C\text{-}4}$ 83.1, $\delta_{C\text{-}5}$ 74.5, $\delta_{C\text{-}6}$ 64.1) and β-D-Gal*f*1Me ($\delta_{C\text{-}1}$ 109.9, $\delta_{C\text{-}2}$

Table 2
^{1}H NMR [a,b] and ^{13}C NMR [c] chemical shifts of S3 native EPS (n-EPS) and O-deacetylated EPS (dAc-EPS), recorded in D_2O at 80 °C for ^{1}H and at 67 °C for ^{13}C [d]

Residue	Proton	n-EPS	dAc-EPS	Carbon	n-EPS	dAc-EPS
A	H-1	4.699	4.696	C-1	104.8 (164)	104.8 (163)
	H-2	3.79	3.77	C-2	70.2	70.3
	H-3	3.79	3.78	C-3	78.3	78.5
	H-4	4.13	4.11	C-4	66.1	66.1
	H-5	3.69	3.68	C-5	75.3	75.4
	H-6a	3.7–3.8 [e]	3.7–3.8 [e]	C-6	61.4	61.4
	H-6b	3.7–3.8 [e]	3.7–3.8 [e]			
B	H-1	5.03	5.031	C-1	108.1 (177)	108.1 (177)
	H-2	4.09	4.09	C-2	78.4	78.5
	H-3	4.06	4.06	C-3	77.5	77.5
	H-4	3.99	3.98	C-4	84.0	84.0
	H-5	3.84	3.84	C-5	71.5	71.6
	H-6a	3.73	3.71	C-6	63.3	63.4
	H-6b	3.66	3.66			
B′	H-1	5.15		C-1	105.5 (179)	
	H-2	4.958		C-2	84.0	
	H-3	4.22		C-3	75.9	
	H-4	4.05		C-4	84.2	
	H-5	3.86		C-5	71.0	
	H-6a	3.74		C-6	63.0	
	H-6b	3.67				
	O-acetyl	2.148		*O*-acetyl	20.5	
C	H-1	5.05	5.051	C-1	102.3 (174)	102.4 (174)
	H-2	4.26	4.26	C-2	67.7	67.7
	H-3	3.86	3.85	C-3	77.3	77.2
	H-4	3.590	3.590	C-4	71.2	71.2
	H-5	3.78	3.77	C-5	69.7	69.6
	H-6	1.31	1.31	C-6	17.0	17.1
D	H-1	5.16	5.16	C-1	97.0 (172)	97.0 (171)
	H-2	4.09	4.09	C-2	67.9	68.0
	H-3	4.11	4.11	C-3	79.5	79.6
	H-4	4.28	4.28	C-4	69.6	69.7
	H-5	4.381	4.382	C-5	69.7	69.8
	H-6a	3.90	3.90	C-6	66.9	67.0
	H-6b	3.71	3.70			
E	H-1	5.17	5.17	C-1	96.0 (176)	96.0 (176)
	H-2	3.99	3.98	C-2	74.5	74.6
	H-3	4.10	4.11	C-3	69.8	69.8
	H-4	4.06	4.06	C-4	70.2	70.3
	H-5	4.24	4.24	C-5	71.5	71.6
	H-6a	3.76	3.76	C-6	61.4	61.4
	H-6b	3.76	3.76			
F	H-1	5.245	5.246	C-1	100.9 (177)	100.9 (177)
	H-2	4.10	4.09	C-2	81.6	81.7
	H-3	3.90	3.89	C-3	nd	70.8
	H-4	3.506	3.507	C-4	nd	72.9
	H-5	3.72	3.71	C-5	nd	69.8
	H-6	1.33	1.33	C-6	17.0	17.1

[a] In ppm relative to the signal of internal acetone at δ 2.225.
[b] Accurate ^{1}H chemical shift values obtained from 1D spectra are represented with three decimals, whereas ^{1}H chemical shift values obtained from 2D spectra are depicted with two decimals.
[c] In ppm relative to the α anomeric signal of external [1-^{13}C]glucose at δ 92.9.
[d] $^{1}J_{C\text{-}1,H\text{-}1}$ values (Hz) are included in parentheses.
[e] Assigned from ^{13}C–^{1}H HSQC spectra.

81.3, δ_{C-3} 78.4, δ_{C-4} 84.7, δ_{C-5} 71.7, δ_{C-6} 63.6)[21] showed this residue to be terminal β-Gal*f*. The downfield chemical shift of **E** C-2 (δ 74.6) demonstrated residue **E** to represent the 2-substituted α-Gal*p* residue (α-D-Gal*p*1Me, δ_{C-2} 69.2). The downfield chemical shifts for C-3 (δ 77.2) of residue **C** and C-2 (δ 81.7) of residue **F** indicate that these α-Rha*p* units are 3- and 2-substituted, respectively (α-L-Rha*p*1Me, δ_{C-2} 71.0, δ_{C-3} 71.3). Finally, residue **D** could be assigned as the 3,6-substituted α-Gal*p* unit, since the **D** C-3 and **D** C-6 signals (δ_{C-3} 79.6, δ_{C-6} 67.0) are shifted downfield in comparison to their methyl aldosides (α-D-Gal*p*1Me, C_{C-3} δ 70.5, C_{C-6} δ 62.2).

The sequence of the monosaccharides in the polysaccharide repeating unit was determined by means of a NOESY experiment (Fig. 4). On the NOESY **C** H-1 track of dAc-EPS an interresidual connectivity with **F** H-2 was in accordance with the **C**(1→2)**F** sequence. A well-resolved NOE between **F** H-1 and **E** H-2

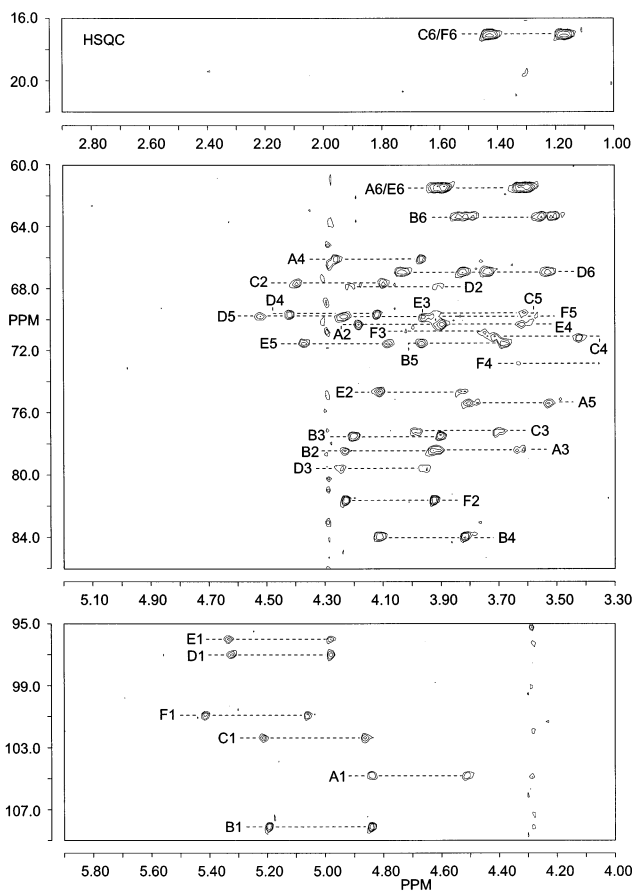

Fig. 3. 500-MHz 2D $^{13}C-^{1}H$ undecoupled HSQC spectrum of dAc-EPS, recorded in D_2O at 67 °C. A1 stands for the set of cross-peaks between H-1 and C-1 of residue **A**, etc.

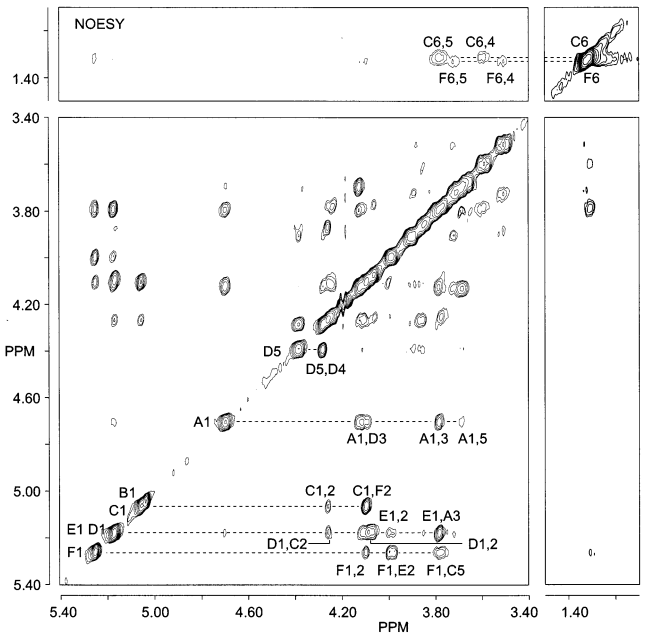

Fig. 4. 500-MHz 2D NOESY spectrum (mixing time 200 ms) of dAc-EPS, recorded in D_2O at 80 °C. F1 corresponds to the diagonal peak belonging to residue **F** H-1; F1,2 refers to an intraresidual cross-peak between **F** H-1 and **F** H-2, and F1,E2 means an interresidual connectivity between **F** H-1 and **E** H-2, etc.

was observed, revealing a **F**(1→2)**E** linkage. The NOE between **F** H-1 and **C** H-5 reflects the closeness in space of these protons in the **C**(1→2)**F**(1→2)**E** sequence. The interresidual connectivity between **E** H-1 and **A** H-2,3 indicated an **E**(1→3)**A** linkage since carbon chemical shifts revealed residue **A** to be substituted at O-3. The NOE between **A** H-1 and **D** H-3 demonstrated an **A**(1→3)**D** linkage. Furthermore, an NOE between **D** H-1 and **C** H-2 was observed. This NOE represents a **D**(1→3)**C** linkage, since methylation analysis in combination with carbon chemical shifts demonstrated residue **C** to be 3-substituted. The observation of such non-glycosidic NOE cross-peaks has been reported previously for the α-D-Gal*p*-(1→3)-α-L-Rha*p* linkage in the EPS of *S. thermophilus* Rs and Sts.[18] The **B**(1→6)**D** linkage determined by partial acid hydrolysis and methylation analysis, could not be confirmed by the NOESY experiment.

The intraresidual connectivities in the NOESY spectrum confirm the anomeric configurations of the various monosaccharide residues in the polysaccharide.

By combining the various analytical data described above, the structure of the repeating

unit of the EPS produced by *S. thermophilus* S3 can be illustrated as:

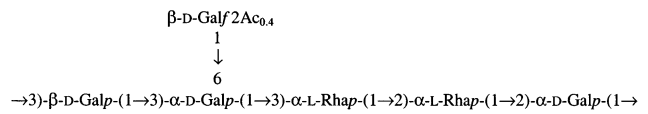

Concluding remarks.—In this paper, the complete elucidation of the structure of the EPS isolated from *S. thermophilus* S3 grown in skimmed milk is described. Several EPSs produced by strains of *S. thermophilus* have been isolated from yogurt, or related media, and their structures studied.[15–18] A number of the EPSs are structurally related polysaccharides and include the EPSs produced by *S. thermophilus* Sfi12,[17] OR 901,[16] Rs,[18] Sts,[18] and S3, of which the OR 901, Rs and Sts EPSs have identical repeating units. The EPSs are characterized by the presence of a pentameric backbone containing a →3)-α-D-Gal*p*-(1→3)-α-L-Rha*p*-(1→2)-α-L-Rha*p*-(1→2)-α-D-Gal*p*-(1→3)-Hex*p*-(1→ sequence, wherein the fifth residue differs by the presence of α-D-Glc*p* for Sfi12, α-D-Gal*p* for OR 901, Rs and Sts, and β-D-Gal*p* for the EPS produced by S3. Furthermore, the EPSs differ in the attachment site of the side chain, as well as in the composition of the side chain.

Although the EPSs produced by several *S. thermophilus* strains share structural features, strains producing EPS with only minor differences in the primary structure of the repeating unit (e.g. single monosaccharide replacement, molecular size) are excellent probes to obtain insight into the relationship between physical properties, such as ropiness, and the structure of the EPS. In this regard, research performed towards biosynthetic engineering techniques as well as genetic engineering techniques to tailor EPSs produced by lactic acid bacteria may assist in creating structural diversity in polysaccharides allowing the establishment of the structure–function relationship of EPS produced by lactic acid bacteria.

3. Experimental

Organism and culture conditions.—*S. thermophilus* S3 is a highly ropy strain obtained from NIZO food research (Ede, The Netherlands). The cultivation of *S. thermophilus* S3 was performed in pasteurized reconstituted skimmed milk as described.[18]

Exopolysaccharide concentration.—The concentration of exopolysaccharide was determined by HP-GPC with RI-detection as previously described.[18]

Isolation and purification of the exopolysaccharide.—To the milk culture, trichloroacetic acid was added to a final concentration of 4% (w/w). After stirring for 1 h, cells and precipitated proteins were removed by centrifugation (2 × 30 min at 16,300*g*, 4 °C). EPS was precipitated from the supernatant by addition of 2 vol of EtOH (4 °C). An aq solution of the precipitated material was extensively dialyzed against running tap water and after the removal of insoluble material by centrifugation, 2 vol of EtOH were added. The precipitate formed was redissolved in water, and purified by a precipitation with 50% (v/v) acetone.

Molecular mass determination.—The average molecular mass of n-EPS was determined by using a combination of gel-permeation chromatography, static light scattering, and differential refraction analysis, as described.[23]

Gas-liquid chromatography and mass spectrometry.—GLC analyses were performed on a Chrompack CP9002 gas chromatograph equipped with a CP-Sil 5CB fused silica capillary column (25 m × 0.32 mm, Chrompack) or a CP-Sil 43CB fused silica capillary column (25 m × 0.25 mm, Chrompack). GLC–MS analyses were carried out on a MD800/8060 system (Fisons instruments; electron energy, 70 eV), using a CP-Sil 5CB fused silica capillary column (25 m × 0.25 mm, Chrompack). Both GLC and GLC–MS analyses were performed under conditions described previously.[18] Positive-ion mode nanoES-CID tandem mass spectra were obtained on a Micromass Q-TOF hybrid tandem mass spectrometer equipped with a nanospray ion source (Bijvoet Center, Department of Biomolecular Mass Spectrometry) essentially according to Ref. 24. Argon was used as collision gas with collision energy of approximately 50 eV. Fragment ions were labeled according to the nomenclature of Domon and Costello.[25]

Monosaccharide and methylation analysis.—For monosaccharide analysis, the dry polysac-

charide was subjected to methanolysis, followed by trimethylsilylation and GLC analysis as described.[26,27] The absolute configuration of the monosaccharides was determined according to Refs. 28 and 29. For methylation analysis, polysaccharides were permethylated using CH_3I and solid NaOH in Me_2SO as described previously.[30] Subsequently, the methylated saccharides were hydrolyzed with 2 M CF_3COOH (2 h, 120 °C) and reduced with $NaBD_4$. After neutralization and removal of boric acid by coevaporation with MeOH, the mixtures of partially methylated alditols were acetylated with Ac_2O (3 h, 120 °C), and analyzed by GLC and GLC–MS.[26,31]

Periodate oxidation.—To a solution of polysaccharide (30 mg) in 0.1 M NaOAc buffer (30 mL, pH 3.9), $NaIO_4$ was added to a final concentration of 50 mM, and the mixture was kept in the dark for 5 days at 4 °C. Excess of periodate was destroyed by the addition of ethylene glycol (2 mL) after which the solution was dialyzed against tap water. The oxidized polysaccharide was reduced with $NaBH_4$ (4 h, 20 °C), and permethylated as described above. The obtained permethylated material was subsequently hydrolyzed (0.5 M CF_3COOH, 75 min, 100 °C), reduced with $NaBD_4$ (4 h, 20 °C), and permethylated using CD_3I.

O-Deacetylation of the polysaccharide.—Native polysaccharide (30 mg) was O-deacetylated by treatment with aq 5% NH_4OH (30 mL) for 8 h at rt. The O-deacetylated polysaccharide was recovered by lyophilization.

NMR spectroscopy.—Prior to NMR spectroscopic analysis, samples were exchanged twice in 99.9 atom% D_2O (Isotec) with intermediate lyophilization, and finally dissolved in 99.96 atom% D_2O (Isotec). The pH of the samples was adjusted to 7.0 using NaOD. 1D and 2D NMR spectra were recorded on a Bruker AMX-500 spectrometer (Bijvoet Center, Department of NMR Spectroscopy). The HOD signal was suppressed either by applying a WEFT pulse sequence[32] in 1D ^1H NMR experiments, or by presaturation for 0.8–1 s in 2D experiments. Chemical shifts are expressed in ppm by reference to internal acetone (δ 2.225) for ^1H or to the α anomeric signal of external [1-^{13}C]glucose ($\delta_{C\text{-}1}$ 92.9) for ^{13}C. Homonuclear NMR experiments were recorded at a probe temperature of 80 °C and heteronuclear NMR experiments at a probe temperature of 67 °C, using a spectral width of 4032 and 16350 Hz for ^1H and ^{13}C, respectively. Resolution enhancement of the spectra was performed by a Lorentzian-to-Gaussian transformation and when necessary, a fourth-order polynomial baseline correction was performed. 2D TOCSY spectra were recorded using a 'clean' MLEV-17 mixing sequence with an effective spin-lock time of 20–150 ms. 2D NOESY experiments were performed with a mixing time of 200 ms, and the natural abundance ^{13}C–^1H 2D HSQC experiment was recorded without decoupling during acquisition of the ^1H FID. All NMR data were processed using TRITON (Bijvoet Center, Department of NMR Spectroscopy) or Bruker UXNMR software.

Acknowledgements

This study was supported by the PBTS Research Program with financial aid from the Ministry of Economic Affairs and by the Integral Structure Plan for the Northern Netherlands from the Dutch Development Company. The authors thank F. Kingma (NIZO Food Research, Ede, The Netherlands) for cultivation of *S. thermophilus* S3 and for HP-GPC analysis, R. Tuinier (NIZO Food Research, Ede, The Netherlands) for molecular mass analysis, and C. Versluis (Bijvoet Center, Department of Biomolecular Mass Spectrometry, Utrecht University, The Netherlands) for recording the ES-MS/MS spectra.

References

1. Sutherland, I. W. *Trends Biotechnol.* **1998**, *16*, 41–46.
2. Robijn, G. W.; Gutiérrez Gallego, R.; van den Berg, D. J. C.; Haas, H.; Kamerling, J. P.; Vliegenthart, J. F. G. *Carbohydr. Res.* **1996**, *288*, 203–218.
3. Gruter, M.; Leeflang, B. R.; Kuiper, J.; Kamerling, J. P.; Vliegenthart, J. F. G. *Carbohydr. Res.* **1993**, *239*, 209–226.
4. Yamamoto, Y.; Murosaki, S.; Yamauchi, R.; Kato, K.; Sone, Y. *Carbohydr. Res.* **1994**, *261*, 67–78.
5. Yamamoto, Y.; Nunome, T.; Yamauchi, R.; Kato, K.; Sone, Y. *Carbohydr. Res.* **1995**, *275*, 319–332.

6. Robijn, G. W.; Thomas, J. R.; Haas, H.; van den Berg, D. J. C.; Kamerling, J. P.; Vliegenthart, J. F. G. *Carbohydr. Res.* **1995**, *276*, 137–154.
7. Staaf, M.; Widmalm, G.; Yang, Z.; Huttunen, E. *Carbohydr. Res.* **1996**, *291*, 155–164.
8. Stingele, F.; Lemoine, J.; Neeser, J.-R. *Carbohydr. Res.* **1997**, *302*, 197–202.
9. Robijn, G. W.; Wienk, H. L. J.; van den Berg, D. J. C.; Haas, H.; Kamerling, J. P.; Vliegenthart, J. F. G. *Carbohydr. Res.* **1996**, *285*, 129–139.
10. van Geel-Schutten, G. H.; Faber, E. J.; Smit, E.; Bonting, K.; Smith, M. R.; ten Brink, B.; Kamerling, J. P.; Vliegenthart, J. F. G.; Dijkhuizen, L. *Appl. Environ. Microbiol.* **1999**, *65*, 3008–3014.
11. Vanhaverbeke, C.; Bosso, C.; Colin-Morel, P.; Gey, C.; Gamar-Nourani, L.; Blondeau, K.; Simonet, J.-M.; Heyraud, A. *Carbohydr. Res.* **1998**, *314*, 211–220.
12. Robijn, G. W.; van den Berg, D. J. C.; Haas, H.; Kamerling, J. P.; Vliegenthart, J. F. G. *Carbohydr. Res.* **1995**, *276*, 117–136.
13. Nakajima, H.; Hirota, T.; Toba, T.; Itoh, T.; Adachi, S. *Carbohydr. Res.* **1992**, *224*, 245–253.
14. Gruter, M.; Leeflang, B. R.; Kuiper, J.; Kamerling, J. P.; Vliegenthart, J. F. G. *Carbohydr. Res.* **1992**, *231*, 273–291.
15. Doco, T.; Wieruszeski, J.-M.; Fournet, B.; Carcano, D.; Ramos, P.; Loones, A. *Carbohydr. Res.* **1990**, *198*, 313–321.
16. Bubb, W. A.; Urashima, T.; Fujiwara, R.; Shinnai, T.; Ariga, H. *Carbohydr. Res.* **1997**, *301*, 41–50.
17. Lemoine, J.; Chirat, F.; Wieruszeski, J.-M.; Strecker, G.; Favre, N.; Neeser, J.-R. *Appl. Environ. Microbiol.* **1997**, *63*, 3512–3518.
18. Faber, E. J.; Zoon, P.; Kamerling, J. P.; Vliegenthart, J. F. G. *Carbohydr. Res.* **1998**, *310*, 269–276.
19. Aspinall, G. O. In *The Polysaccharides*; Aspinall, G. O., Ed.; Academic: New York, 1982; Vol. 1, pp. 81–86.
20. Brüll, L. P.; Kovácik, V.; Thomas-Oates, J. E.; Heerma, W.; Haverkamp, J. *Rapid Commun. Mass Spectrom.* **1998**, *12*, 1520–1532.
21. Bock, K.; Pedersen, C. *Adv. Carbohydr. Chem. Biochem.* **1983**, *41*, 27–66.
22. Kol, O.; Wieruszeski, J.-M.; Strecker, G.; Fournet, B.; Zalisz, R.; Smets, P. *Carbohydr. Res.* **1992**, *236*, 339–344.
23. Tinland, B.; Mazet, J.; Rinaudo, M. *Makromol. Chem.* **1988**, *9*, 69–73.
24. Samuelsen, A. B.; Cohen, E. H.; Paulsen, B. S.; Brüll, L. P.; Thomas-Oates, J. E. *Carbohydr. Res.* **1999**, *315*, 312–318.
25. Domon, B.; Costello, C. E. *Glycoconjugate J.* **1988**, *5*, 397–409.
26. Chaplin, M. F. *Anal. Biochem.* **1982**, *123*, 336–341.
27. Kamerling, J. P.; Vliegenthart, J. F. G. In *Mass Spectrometry*; Lawson, A. M., Ed. Clinical biochemistry — principles, methods, applications. Walter de Gruyter: Berlin, 1989; Vol. 1, pp. 176–263.
28. Gerwig, G. J.; Kamerling, J. P.; Vliegenthart, J. F. G. *Carbohydr. Res.* **1978**, *62*, 349–357.
29. Gerwig, G. J.; Kamerling, J. P.; Vliegenthart, J. F. G. *Carbohydr. Res.* **1979**, *77*, 1–7.
30. Ciucanu, I.; Kerek, F. *Carbohydr. Res.* **1984**, *131*, 209–217.
31. Jansson, P.-E.; Kenne, L.; Liedgren, H.; Lindberg, B.; Lönngren, J. *Chem. Commun. Univ. Stockholm* **1976**, *8*, 1–74.
32. Hård, K.; van Zadelhoff, G.; Moonen, P.; Kamerling, J. P.; Vliegenthart, J. F. G. *Eur. J. Biochem.* **1992**, *209*, 895–915.